Advanced Materials Research, Vols 89--91, 2010, 651-656

Crystallographic Texture of Induction-welded and Heat-treated Pipeline Steel

P. Yan[1,a], Ö. E. Güngör[2,b] , P. Thibaux[2,c] and H. K. D. H. Bhadeshia[1,d]

[1]University of Cambridge, Materials Science and Metallurgy, Cambridge CB2 3QZ, U.K.

[2]ArcelorMittal R&D Gent, OCAS NV, Pres. J. F. Kennedylaan 3, BE-9060 Zelzate, Belgium

[a]py210@cam.ac.uk, [b]ozlem.esma.gungor@arcelormittal.com, [c]philippe.thibaux@arcelormittal.com, [d]hkdb@cam.ac.uk

Keywords: crystallographic texture; pipeline steel; induction welding; induction heat-treatment.

Abstract. Large-diameter steel pipes are produced by induction seam-welding followed by induction-assisted heat treatment. The microstructure and distribution of crystal orientations have been studied and related to the mechanical properties of the welded regions. The welding and heat-treatment process leads to a microstructure, a simple observation of which can not explain the observed variations in toughness in the vicinity of the welding joint, because the crystallographic grain size, which represents the scale of similarly oriented adjacent grains, is much coarser than the ordinary grain size. Furthermore, heating the affected zone into the austenite phase field followed by cooling does not completely eliminate the coarse regions of similarly oriented grains. The consequences of this on mechanical properties are discussed.

Introduction

Pipes for oil and gas transmission are made from low-alloy steels designated X60, X65, X70 etc. depending on the strength and toughness required and the intended application [1–3]. One method of fabricating pipes from these materials is by high–frequency induction seam–welding. Pipes some 18 m in length, 500 mm in diameter and 12.7 mm in thickness are routinely manufactured in this way [4]. The toughness of line pipes is paramount in their suitability for application [5–7]. The joint resulting from induction welding is quite narrow, with a central 2 mm wide region, but it represents a source of weakness, so the welding process is immediately followed by induction heat treatment. The intention of the latter is to refine the microstructure by reaustenisation at a lower temperature than the peak temperature achieved during welding. Although the heat–treatment improves the toughness of the welded region, the increase is not as large as might be expected from the reduction in the scale of the microstructure. The purpose of the present work was to understand this insensitivity of the toughness to heat–treatment.

Experimental Procedures

The chemical composition of the steel is Fe–0.041C–1.1Mn–0.18Si wt% with micro–alloying of Nb and V. Details of the heat-treatment are proprietary, but it involves rapid heating to above a temperature at which austenite can form, and subsequently fast cooling.

Specimens were obtained from different stages of the manufacturing process: the unaffected base metal, the pipe just after welding, and finally, the pipe after welding and heat–treatment. Samples were cut normal to the welding direction which is parallel to the rolling direction of the steel and to the length of the pipe. Some were flattened to make non–standard cross–weld Charpy test specimens of size 55 × 6.7 × 10 mm. The tests were conducted according to the standard ISO 148-1.

Metallographic specimens were prepared in the usual way by grinding, polishing and etching (using 2% nital). Orientation imaging requires scratch–free surfaces so the metallographic samples were finished using colloidal silica. Scanning electron microscopy was conducted on a Camscan MX2600 equipped with a field emission gun and an Electron back scattered diffraction (EBSD) system, with HKL Channel 5 software. The orientation images were taken at an operating voltage of 25 kV, a working distance of 30 mm and a tilt angle of 70°.

Microstructural Characterisation

Pipelines steels are normally hot–rolled at elevated temperatures in the austenitic condition followed by accelerated cooling [8, 9]. Because of the low solute–content in the steel, the first phase to form in spite of the rapid cooling is allotriomophic ferrite (α) which enriches the remaining austenite with carbon; the later eventually transforms into fine pearlite. It is not surprising therefore that the microstructure of the steel prior to welding consists predominantly of allotriomorphic ferrite with a very small fraction of pearlite (Fig. 1a). This kind of a microstructure is henceforth referred to as 'base metal'. The macroscopic form of the weld, together with its key microstructural zones, is illustrated in Figure 1b. There are four zones of interest, the base metal, thermomechanically affected zone (TMAZ), heat–affected zone (HAZ) and at the fusion line – their microstructures are illustrated in Fig. 2.

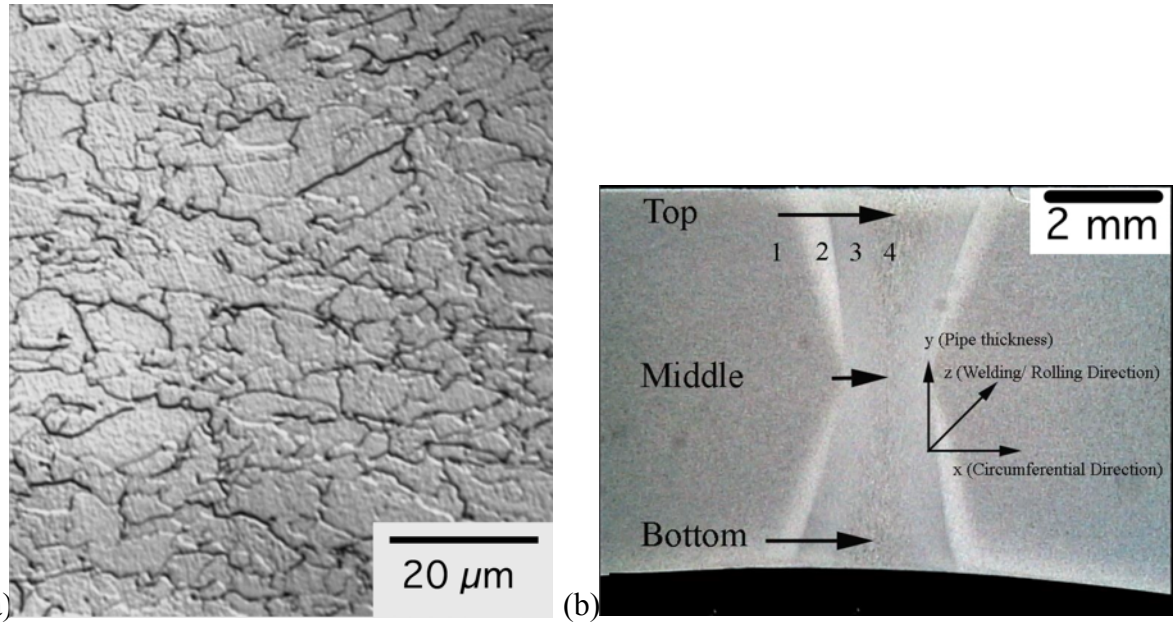

(a) (b)

Figure 1: (a) Steel prior to welding. (b) Zones associated with weld: 1–base metal, 2–TMAZ, 3–HAZ, and 4–fusion line.

Welding in the present context is in the solid–state, with the butting edges of the pipe being pushed together whilst they are hot and plastic, thus giving rise to flow which serves two purposes: first, to expel undesirable oxides from the weld zone, and secondly to form a metallurgical bond by breaking up the interface between the edges. There is therefore a TMAZ where remnants of the deformation associated with the welding process are retained. Thus, it has a structure similar to that of the base metal, except that the shapes of the ferrite grains are anisotropic, aligned along the direction of metal flow, Fig. 2a. It is possible that this alignment is purely due to the deformation of ferrite, but it is possible that the morphology observed is a consequence of the severe pancaking of the austenite [10, 11] before it transforms into ferrite.

The HAZ of the weld consists mainly of equiaxed allotriomorphic ferrite which has reformed from the grains which become austenite and then dynamically recrystallises Fig. 2b. The gradients

of microstructure expected in the wide HAZ of conventional fusion welds, i.e., tempered, intercritically heated and fully austenitised regions, are not obvious, partly because of the narrow dimensions of the zone but also because the steel has such a low solute–content.

The microstructure at and adjacent to the fusion line was interesting, consisting of a mixture of grain boundary allotriomorphs of ferrite, Widmanstätten ferrite and minute amounts of pearlite between the ferrite plates, Fig. 2c. This is a direct consequence of the fact that the austenite grains here are expected to be coarser (this can be seen by looking at the allotriomorphs which are located at the austenite grain boundaries). It is well–known that coarse austenite grains favour the formation of Widmanstätten ferrite [12–14].

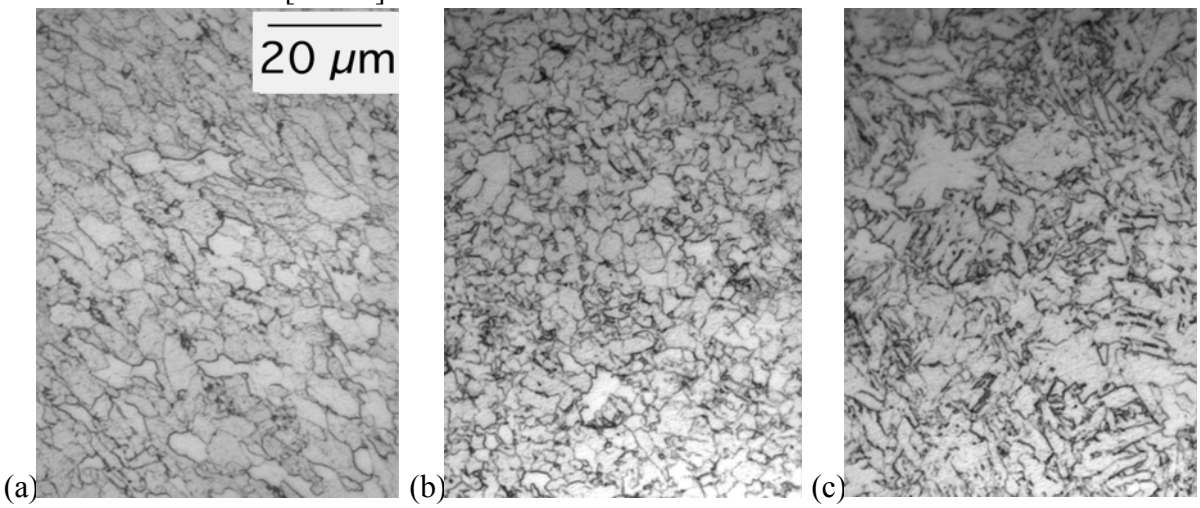

Figure 2: (a) TMAZ, (b) HAZ and (c) fusion line.

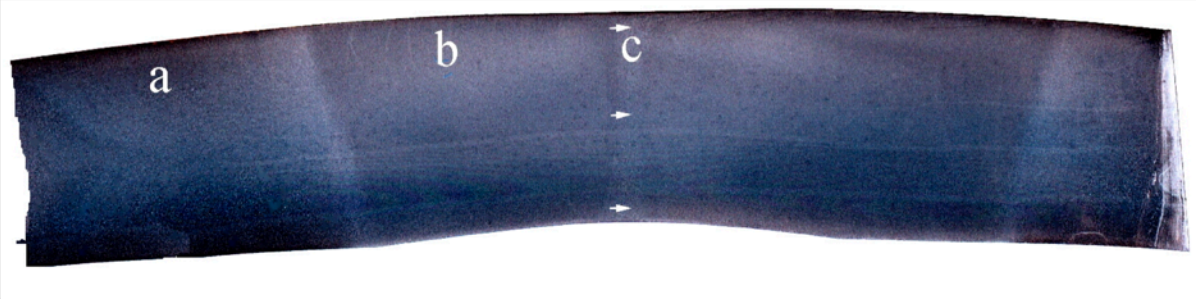

Figure 3: Weld joint segment after post welding heat treatment (PWHT). The pipe is about 1 cm thick. ‘a’ represents the base metal, ‘b’ the broadened affected zone and ‘c’ identifies the original location of the weld.

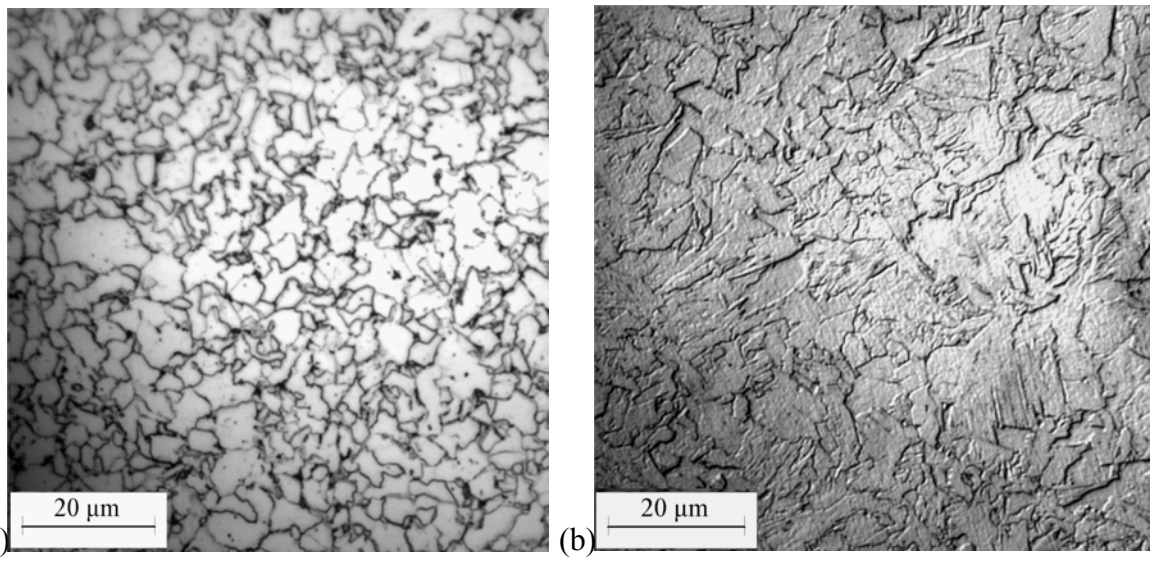

(a) (b)

Figure 4: Microstructure of weld zone following heat treatment. (a) Affected zone, (b) at location of original weld.

The post–weld induction heat–treatment significantly broadens the affected zone as shown in Fig. 3. Micrographs corresponding to the affected zone and the region representing the original location of the weld ('c') are shown in Fig. 4. The fact that the induction heat–treatment does not form austenite means that the microstructure of the affected zone still consists of allotriomorphic ferrite and pearlite, Fig. 4a. Vestiges of the original welding joint remained after heat treatment, Fig. 4b, although the microstructure of the weld becomes uniform as shown in Fig. 3c. The alignment of ferrite grains in the former TMAZ has been annealed out, no zone can be differentiated.

Charpy Impact Data

The toughness is illustrated in Fig. 5. Samples from the base metal, as-welded and samples after post welding heat treatment (PWHT) with the V-notches located on the fusion line, 1 mm (FL+1) and 3 mm (FL+3) apart from the fusion line were tested. Each point in Fig. 5 is the average value of three test results. The Charpy energy of the sample after PWHT was significantly higher than the as-welded sample when the V-notches were located 1 or 3 mm away from the joint. However, when the V-notch was located on the joint, the improvement in toughness from the heat treatment was not so obvious with no enhancement noted for the test temperature of −40 °C, as shown in Fig. 5.

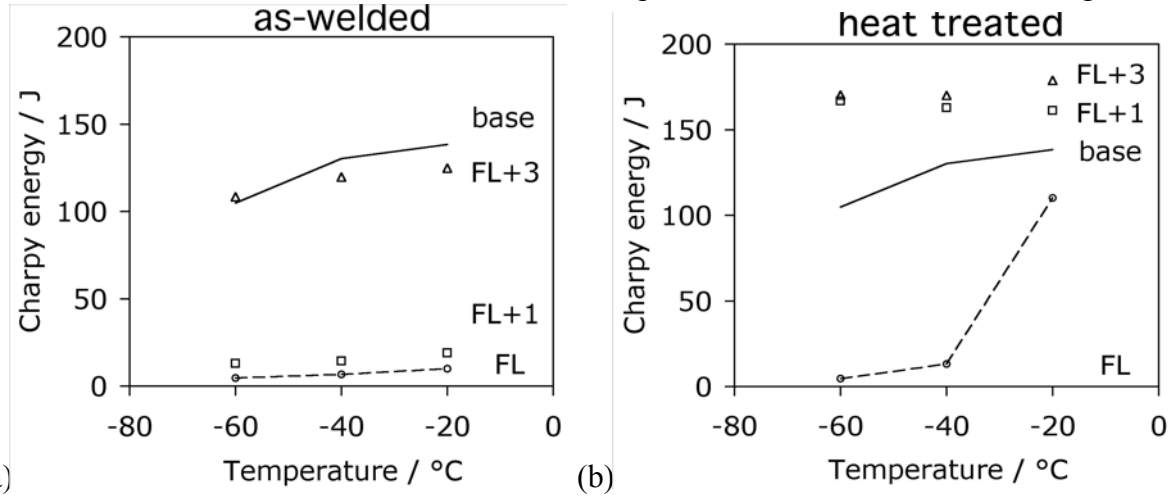

(a) (b)

Figure 5: Charpy impact test energy as a function of temperature. 'FL' designates the Charpy notch located at the fusion surface, and 'FL+1' when the notch is 1 mm from the fusion surface. (a) As welded condition. (b) Welded and heat treated.

Crystallographic Characterisation

There is no clear microstructural indication for the lack of toughness improvement at the fusion line in spite of the heat treatment. EBSD was used with scanning at a step size of 0.2 μm to search for clues because it is known that the crystallographic grain size can be different from that measured using optical microscopy [15, 16]. In the orientation images presented below, blue, green and red colours represent the {111}, {110}, and {001} pole respectively, normal to the plane of the image.

Figure 6 shows that the crystallographic grain size becomes very coarse at the fusion line, even though this is not obvious in the optical microstructure shown in Fig. 2c. This observation was confirmed by looking at the detailed pole figures which are not presented here for brevity.

The coarse crystallographic grain size persisted after heat–treatment as shown for the region near the fusion line in Fig. 7, where the accompanying stereogram shows clusters of grains which are almost identically oriented over regions coarser than 20 μm. These results explain the persistence of low toughness in this region after heat–treatment. Examination of the fracture surface of a broken Charpy specimen revealed fracture facets crossing many grains, and of the same order of magnitude in scale to the clusters of similarly oriented grains, Fig. 8.

The question then arises as to why the austenite texture present just after welding does not vanish during the reaustenisation that occurs in the induction PWHT. There is published work [17] indicating the existence of an austenite memory effect [17] during rapid reaustenisation experiments. An investigation of this will form the basis of future work.

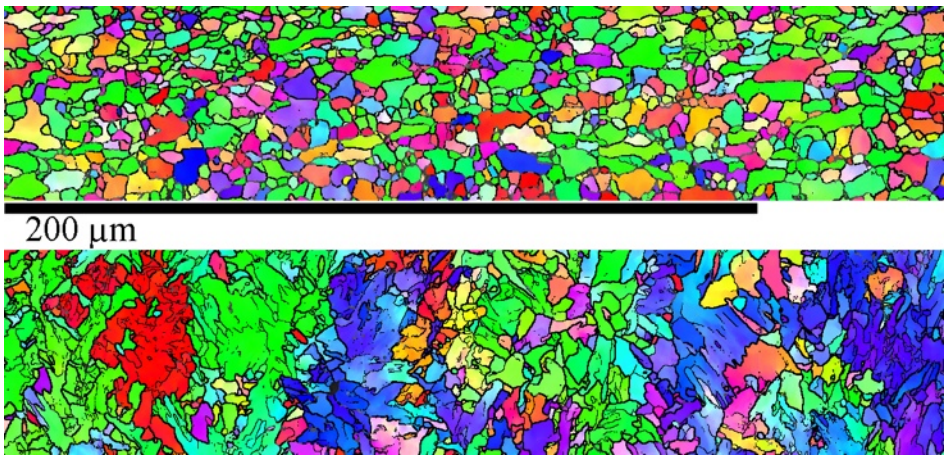

Figure 6: Orientation image along the top line of the as-welded sample. The top part is the base metal and the lower part at and in the vicinity of the fusion line.

Figure 7: Heat treated sample. (a) Orientation image near fusion line. (b) Pole figure showing strong texture.

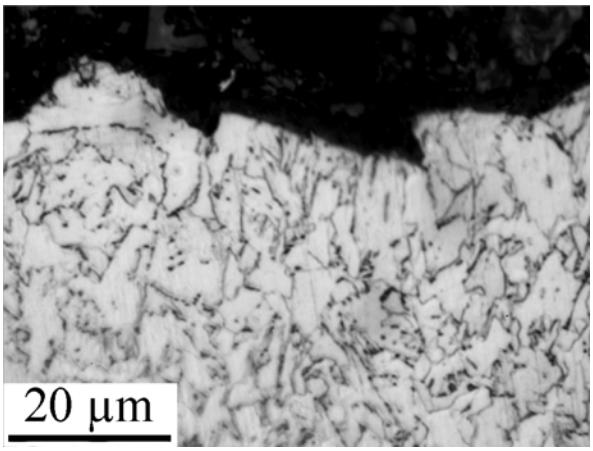

Figure 8: Cross-sectional fracture surface near the V-notch of the charpy sample tested at −40 °C with a V-notch located on the fusion line.

Conclusions

It is found that the low toughness at the position of the fusion line in induction welded samples of the pipe does not vanish thoroughly on post welding heat treatment which involves the austenisation of the weld zone. This is because the crystallographic grain size in that region remains coarse, possibly due to a memory effect.

Acknowledgement

The authors are grateful to ArcelorMittal for financial, material and intellectual support and to Eric Hivert, and David Quidort for helpful discussions.

References

[1] C. Shiga, A. Kamada, T. Hatomura, K. Hirose, J. Junichi, and T. Sekine. Development of large diameter high strength line pipes for low temperature services. Technical Report 4, Kawasaki Steel Technical Report, Kawasaki Steel, Japan, 1981, p. 97–109.

[2] J. Q. Wang, A. Atrens, D. R. Cousens, and N. Kinaev: Journal of Materials Science Vol. 34 (1999), p. 1721.

[3] M. C. Zhao, K. Yang, F. R. Xiao, and Y. Y. Shan: Materials Science & Engineering A Vol. 355 (2003), p. 126.

[4] E. Treiss: 3R International Vol. 20(11) (1981), p. 627.

[5] J. G. Williams, C. R. Killmore, F. J. Barbaro, A. Meta, and L. Fletcher, in: *Microalloying '95 Conference Proceedings*, edited by M. Korchynsky, A. J. DeArdo, P. Repasi, and G. Tither ISS–AIME, Warrendale, Pennsylvania (1995), p. 117.

[6] C. Yu: Tube International March (1996), p. 153.

[7] N. Pradhan, N. Banerjee, B. B. Reddy, S. K. Sahay, D. S. Basu, P. K. Bhor, S. Das, and S. Bhattyacharya: Scandinavian Journal of Metallurgy Vol. 34 (2005), p. 232.

[8] J. P. Benedict, R. Anderson, S. J. Klepeis, and M. Chaker, in: volume 199 of Materials Research Society Symposium Proceedings (1990), p. 189.

[9] J. G. Williams, C. R. Killmore, F. J. Barbaro, J. Piper, and Fletcher: Materials Forum Vol. 20 (1996), p. 13.

[10] G. R. Speich, L. J. Cuddy, C. R. Gordon, and A. J. DeArdo, in: *Phase Transformations in Ferrous Alloys* edited by A. R. Marder and J. I. Goldstein, TMS–AIME., Warrendale, Pennsylvania, USA (1984), p. 341.

[11] I. Tamura: Trans. ISIJ Vol. 27 (1987), p. 763.

[12] R. L. Bodnar and S. S. Hansen: Metallurgical & Materials Transactions A Vol. 25A (1994), p. 665.

[13] S. Jones and H. K. D. H. Bhadeshia: Acta Materialia Vol. 45 (1997), p. 2911.

[14] S. Jones and H. K. D. H. Bhadeshia: Metallurgical & Materials Transactions A Vol. 28A (1997), p. 2005.

[15] A. Lambert-Perlade, A. F. Gourgues, and A. Pineau: Acta Materialia Vol. 52 (2004), p. 2337.

[16] Y. M. Kim, S. Y. Shu, H. Lee, B. Hwang, S. Lee, and N. J. Kim: Metallurgical &Materials Transactions A Vol. 38 (2007), p. 1731.

[17] S. T. Kimmins and D. J. Gooch: Metal Science Vol. 17 (1983), p. 519.